

# Dynamics of SARS-CoV-2 with Waning Immunity in the UK Population

Thomas Crellen<sup>1,\*</sup>, Li Pi<sup>1</sup>, Emma L. Davis<sup>1</sup>, Timothy M. Pollington<sup>1,2</sup>, Tim C. D. Lucas<sup>1</sup>, Diepreye Ayabina<sup>1</sup>, Anna Borlase<sup>1</sup>, Jaspreet Toor<sup>1</sup>, Kiesha Prem<sup>3</sup>, Graham F. Medley<sup>3</sup>, Petra Klepac<sup>3,†</sup>, and T. Déirdre Hollingsworth<sup>1,†,\*</sup>

<sup>1</sup>Big Data Institute, Old Road Campus, University of Oxford, Oxford, OX3 7LF, UK

<sup>2</sup>MathSys CDT, University of Warwick, Coventry, CV4 7AL, UK

<sup>3</sup>London School of Hygiene and Tropical Medicine, London, WC1E 7HT, UK

<sup>†</sup>Contributed equally

\*Corresponding authors: [thomas.crellen@bdi.ox.ac.uk](mailto:thomas.crellen@bdi.ox.ac.uk) & [deirdre.hollingsworth@bdi.ox.ac.uk](mailto:deirdre.hollingsworth@bdi.ox.ac.uk)

July 24, 2020

## Abstract

The dynamics of immunity are crucial to understanding the long-term patterns of the SARS-CoV-2 pandemic. While the duration and strength of immunity to SARS-CoV-2 is currently unknown, specific antibody titres to related coronaviruses SARS-CoV and MERS-CoV have been shown to wane in recovered individuals, and immunity to seasonal circulating coronaviruses is estimated to be shorter than one year. Using an age-structured, deterministic model, we explore different potential immunity dynamics using contact data from the UK population. In the scenario where immunity to SARS-CoV-2 lasts an average of three months for non-hospitalised individuals, a year for hospitalised individuals, and the effective reproduction number ( $R_t$ ) after lockdown is 1.2 (our worst case scenario), we find that the secondary peak occurs in winter 2020 with a daily maximum of 409,000 infectious individuals; almost three-fold greater than in a scenario with permanent immunity. Our models suggests that longitudinal serological surveys to determine if immunity in the population is waning will be most informative when sampling takes place from the end of the lockdown until autumn 2020. After this period, the proportion of the population with antibodies to SARS-CoV-2 is expected to increase due to the secondary peak. Overall, our analysis presents considerations for policy makers on the longer term dynamics of SARS-CoV-2 in the UK and suggests that strategies designed to achieve herd immunity may lead to repeated waves of infection if immunity to re-infection is not permanent.

## 1 Introduction

As of 1<sup>st</sup> July 2020, SARS-CoV-2 has infected at least 10 million people worldwide and resulted in over 500,000 deaths [1, 2]. Following the initial outbreak from a live animal market in Wuhan, China [3], the United Kingdom (UK) has been among the countries most severely affected; reporting over 310,000 cases and 44,000 deaths, which is among the highest per-capita rates [2, 4]. Since 23<sup>rd</sup> March, nationwide non-pharmaceutical interventions (lockdown) have been in place to reduce social contacts by closing schools and shops; encouraging home working; and social distancing in public places. Similar measures have been in place in other European countries since late February 2020 with restrictions easing in France, Germany and Italy from May 2020. Within the European picture of disease control strategies, Sweden has been an outlier by placing fewer restrictions on social mixing while aiming to build up immunity in the population [5].

Following infection with the virus, hospitalised patients have an acute immune response where virus-specific IgM and IgG antibodies titres reach a maximum 15–21 and 22–27 days respectively after symptom onset [6, 7]. Antibodies raised in hospitalised patients and animal models against SARS-CoV-2 provide protection for at least several weeks following infection [8, 9], suggesting that immediate reinfection with the virus is unlikely. There is limited evidence that hospitalised patients with more severe symptoms show a greater antibody response [6, 9]. Asymptomatic individuals have a weaker IgG and specific antibody response to SARS-CoV-2 and are more likely to become seronegative following convalescence [10]. While the duration of immunity to SARS-CoV-2 is not currently known, antibody titres raised against related coronaviruses SARS-CoV and MERS-CoV have been shown to decay over time [11, 12]. Furthermore, immunity to seasonal circulating coronaviruses has been estimated to last for less than one year [13] and recovered individuals from coronavirus NL63 can become

reinfected [14]. Concerns that immunity to SARS-CoV-2 may also wane have therefore motivated the present study [15].

Dynamic epidemiological models play a major role in shaping the timing and intensity of interventions against SARS-CoV-2 in the UK and elsewhere [16]. Many models or simulations have assumed that infected individuals recover with permanent immunity [16, 17, 18]. In such models the epidemic reaches extinction after running out of infected individuals, although they do not preclude a second wave of infections after lockdown [19]. If immunity wanes over a period of time, or recovered individuals have only partial immunity to re-infection, this substantially alters the dynamics of the system [20]. In the absence of stochastic extinction and demography (births and deaths) in a population with equal mixing where;  $R_0$  is the basic reproduction number;  $\gamma$  is the average duration of infection; and  $\omega$  is the reciprocal of the average duration of immunity; the endemic equilibrium proportion of infected in the population  $I^*$ , is given by  $(R_0 - 1)\omega/\gamma R_0$  and thus, in the absence of interventions, the infection persists indefinitely when  $R_0 > 1$  [21].

In dynamic models which make the assumption of homogeneous mixing in the population, the ‘classic’ herd immunity threshold is given by  $1 - 1/R_0$ . As  $R_0$  for SARS-CoV-2 is generally estimated between 2.4–4 [22, 23, 24], this equates to 58–75% of the population requiring immunity to eventually halt the epidemic. Serological studies conducted in affected countries to-date have reported the proportion of the population with antibodies against SARS-CoV-2 to be much lower than this figure [22, 25]. However, when more realistic non-homogeneous mixing is considered, the observed herd immunity threshold is lower than the classical threshold [26]. Recent studies have considered this question for SARS-CoV-2 [27, 28], with Britton *et al.* noting that the disease-induced herd immunity threshold could be closer to 40% in an age-structured population, rather than the 60% classic herd immunity threshold when  $R_0$  is 2.5 [28]. This phenomenon is driven by individuals that have more contacts, or greater susceptibility to the virus, getting infected earlier on and leaving the susceptible population; thus decelerating the growth of the epidemic.

Kissler *et al.* considered the dynamics of SARS-CoV-2 in the United States with seasonal forcing, homogeneous mixing and waning immunity that could be boosted by exposure to seasonal circulating betacoronaviruses [13]. Under these assumptions, the incidence of SARS-CoV-2 was predicted to rebound in winter months. Here we do not consider seasonality, but rather the dynamics of transmission in an age-structured population with different periods of waning immunity in the context of the UK emerging from lockdown.

We developed a discrete-time gamma delay-distributed (susceptible-exposed-infectious-recovered-susceptible; SEIRS) model, which incorporates current knowledge about the natural history of the virus and the UK population. Our model accounts for symptomatic and asymptomatic transmission, and heterogeneity in both daily contacts and infection susceptibility by age group. We consider different durations of immunity for hospitalised patients (or those with more severe symptoms) compared to non-hospitalised patients (those with less severe symptoms). We use this model to explore a range of scenarios in the UK population in the context of stringent non-pharmaceutical interventions (lockdown) followed by more limited interventions over a two year period from February 2020, and the impact of immunity duration on the longer term disease equilibrium.

## Methods

### Model structure

We use current knowledge of the natural history of the virus to construct a plausible epidemiological model (Figure 1). We extend a previously published deterministic compartmental model which has provided general insights into the dynamics of the epidemic at a national level for a range of scenarios [18]. The general framework of the model is given in Figure 1 and parameter values are shown in Table 1.

### Distributed natural history of infection

The mean latent and infectious periods for SARS-CoV-2 have been estimated as 4.5 days and 3.1 days respectively, using viral load data and the timing of known index and secondary case contacts (Figure 2) [29]. As the probability mass of the latent and infectious period distributions are centred around the mean, we consider that gamma distributions with an integer shape parameter (also known as Erlang distributions), give more realistic waiting times than exponential distributions which have a mode of zero [30, 31, 32].

### Transmissibility and infectivity

Estimates of the transmissibility of the virus in the UK at the beginning of the epidemic have ranged from 2.4–3.8 [23, 33, 34], here we assume that  $R_0$  at the beginning of the epidemic in the UK population is 2.8. Non-pharmaceutical interventions have been shown to bring the effective reproduction number ( $R_t$ ) below one, and in some settings have led to local elimination of the virus [22, 23].

74 Testing performed in closed populations suggests that 40-50% of SARS-CoV-2 infections may be asym-  
 75 ptomatic [35, 36, 37], while data from contact tracing shows transmission can occur from asymptomatic in-  
 76 dividuals [38]. We make the assumption that asymptomatic individuals ( $I^A$ ) have 0.5 the infectiousness of  
 77 symptomatic individuals ( $I^S$ ) [6, 16].

78 The UK population shows variable contact rates by age [39, 40] and, while studies show mixed results,  
 79 evidence is accruing that children have a lower susceptibility to acquiring the infection than adults [41, 42, 43].  
 80 We assume that children ( $\leq 15$  years) have 0.4 times the susceptibility of adults [44].

## 81 Scenarios for immunity

82 We allow the duration of immunity to differ for recovered individuals with severe symptoms that are hospitalised  
 83 ( $R^H$ ) versus those with less severe symptoms that are not hospitalised ( $R^N$ ), as there is evidence from SARS-  
 84 CoV-2 and other coronaviruses that individuals with milder symptoms may have a lower antibody response  
 85 [45]. The average duration of immunity for hospitalised and non-hospitalised individuals varies by scenario and  
 86 is described below.

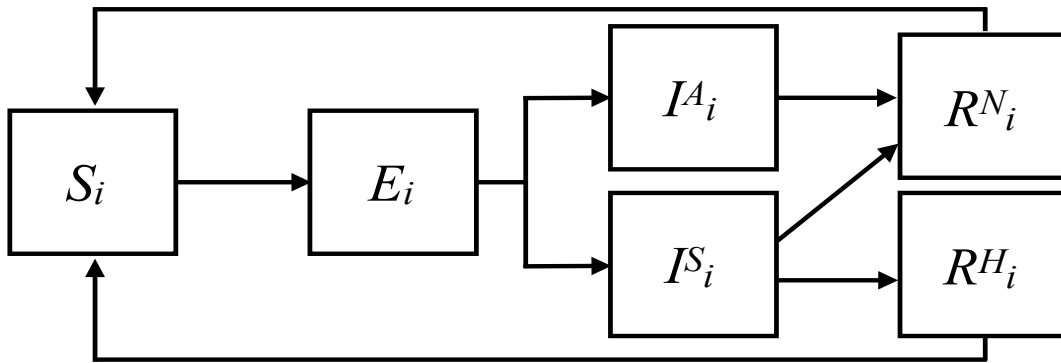


Figure 1: Flow diagram showing SARS-CoV-2 transmission model outline. The disease states are susceptible ( $S$ ), exposed ( $E$ ), symptomatic infectious ( $I^S$ ), asymptomatic infectious ( $I^A$ ), hospitalised recovered ( $R^H$ ), and non-hospitalised recovered ( $R^N$ ). Age group specific parameters are indexed by  $i$ .

## 87 Scenarios for immunity

88 Epidemic transitions for age group  $i$  at time  $t + 1$  are given by:

$$S_{t+1} = S_t(1 - \lambda_t) + f(R_t^N; o, \omega^N) + f(R_t^H; o, \omega^H) \quad (1)$$

$$E_{t+1} = E_t + S_t \lambda_t - f(E_t; m, \sigma) \quad (2)$$

$$I_{t+1}^A = I_t^A + \phi_i f(E_t; m, \sigma) - f(I_t^A; n, \gamma) \quad (3)$$

$$I_{t+1}^S = I_t^S + (1 - \phi_i) f(E_t; m, \sigma) - f(I_t^S; n, \gamma) \quad (4)$$

$$R_{t+1}^N = R_t^N + f(I_t^A; n, \gamma) + \left(1 - \frac{p_i}{\phi_i}\right) f(I_t^S; n, \gamma) - f(R_t^N; o, \omega^N) \quad (5)$$

$$R_{t+1}^H = R_t^H + \frac{p_i}{\phi_i} f(I_t^S; n, \gamma) - f(R_t^H; o, \omega^H) \quad (6)$$

89 The function  $f(x, \alpha, B)$  represents the Erlang delay distribution within classes  $E$ ,  $I^S$ ,  $I^A$ ,  $R^H$  and  $R^N$ ;  
 90 which is achieved by using  $\alpha$  concatenated sub-compartments for each class with rates  $B$  between each sub-  
 91 compartment. If  $n$  individuals enter state  $X$  at time  $t$ , by time  $t + \tau$  there will be remaining  $n(t)(1 - g(\tau, \alpha, B))$ ,  
 92 where  $g(\tau, \alpha, B)$  gives the cumulative Erlang distribution with (integer) shape parameter  $\alpha$  and rate parameter  
 93  $B$ :

$$g(\tau; \alpha, B) = 1 - \sum_{n=0}^{\alpha-1} \frac{1}{n!} e^{-B\tau} (B\tau)^n \quad (7)$$

94 The next generation matrix ( $K = k_{ij}$ ) gives the expected number of secondary infections in age group  $i$   
 95 resulting from contact with an index case in age group  $j$ :

$$k_{ij} = \frac{\beta}{\gamma} \eta_i c_{i,j} (\phi_j v + (1 - \phi_j)) \quad (8)$$

96 The basic reproduction number ( $R_0$ ) is given by the spectral radius  $\rho(K)$  which is the largest absolute  
 97 eigenvalue of  $K$ . The force of infection acting on age group  $i$  at time  $t + 1$  ( $\lambda_{t+1}$ ) is given by:

$$\lambda_{t+1} = \beta \eta_i \sum_{j=1}^{N_a-1} c_{i,j} \frac{I_{j,t}^S + I_{j,t}^A v}{N_j} \quad (9)$$

98 where  $c_{i,j}$  is the average number of daily contacts in the population between age groups  $j$  and  $i$ ;  $N_a$  is the  
 99 number of discrete age groups ( $N_a = 15$ ); and  $N_j$  gives the population size of age group  $j$ . As we specify the  
 100 value of  $R_0$ , the transmission parameter  $\beta$  is left as a free parameter which is scaled to the correct value.

Parameter name	Symbol	Estimate(s)	Details	Reference(s)
Basic reproduction number	$R_0$	2.8	-	Key assumption
Latency period mean	$\sigma$	4.5 days	-	[29, 46, 47]
Latency period shape	$m$	4	-	[29, 46, 47]
Infectious period mean	$\gamma$	3.1 days	-	[29, 46, 47]
Infectious period shape	$n$	2	-	[29, 46, 47]
Immune duration mean non-hospitalised	$\omega^N$	$\infty, 365, 180, 90$ days	Varies by scenario	[11, 45, 48]
Immune duration mean hospitalised	$\omega^H$	$\infty, 365$ days	Varies by scenario	[11, 45, 48]
Immune duration shape	$o$	2	Centres distribution around mean	[11]
$\mathbb{P}(\text{asymptomatic} \mid \text{infection})$	$\phi_i$	$\leq 15$ yrs 0.75 $> 15$ yrs 0.5	Varies by age group $i$	[41]
$\mathbb{P}(\text{hospitalisation} \mid \text{infection})$	$p_i$	0–0.26	Varies by age group $i$	[16, 36]
Effective reproduction number	$R_t$	1.1, 0.8	During lockdown	[49]
		0.9, 1, 1.1, 1.2	After lockdown ends	Key assumption
Contact matrix	$C$ or $c_{ij}$	Varies by age group	BBC survey	[39, 40]
Relative infectiousness of asymptomatic cases	$v$	0.5	-	[16]
Relative age susceptibility	$\eta_i$	$\leq 15$ yrs 0.4 $> 15$ yrs 1	-	[44]

Table 1: Summary of parameter values used in the modelled scenarios of SARS-CoV-2 transmission in the United Kingdom.

## 101 Immunological scenarios

102 Using data and timing of events from the UK epidemic, we explore four scenarios with varying average durations  
 103 of immunity to SARS-CoV-2 (Figure 2).

- 104 S1. **Permanent:** Where immunity is lifelong for both hospitalised ( $R^H$ ) and non-hospitalised ( $R^N$ ) cases.
- 105 S2. **Waning (12 months):** Where immunity is lifelong for hospitalised cases and has an average duration of  
 106 365 days for non-hospitalised cases.
- 107 S3. **Waning (6 months):** Where immunity is lifelong for hospitalised cases and has an average duration of  
 108 180 days for non-hospitalised cases.
- 109 S4. **Short-lived:** Where immunity lasts, on average, 365 days for hospitalised cases and 90 days for non-  
 110 hospitalised cases.

## 111 UK-specific parameterisation

112 All scenarios are initialised with 200 infected individuals in early February 2020. Intervention measures are  
 113 initiated on 23<sup>rd</sup> March (date the UK nationwide lockdown started), with an immediate reduction in the  
 114 effective reproduction number (expected number of secondary cases from an index case at time  $t$ ;  $R_t$ ) to 1.1 for  
 115 a three week period, followed by a further reduction in  $R_t$  to 0.8 until lockdown measures are eased on 15<sup>th</sup> June  
 116 [49]. After this time,  $R_t$  is brought to 0.9, 1, 1.1 or 1.2 until February 2022. We considered the majority of our  
 117 analysis over a, relatively short, two year period to explore the epidemic up to a secondary peak; beyond this  
 118 point the dynamics are likely to be altered depending on further interventions or changes to  $R_t$ . As we simulate  
 119 disease dynamics over a relatively short period of time, we do not consider demography (births and deaths) or  
 120 transitions between age classes (ageing). To obtain equilibrium values, we simulated epidemic trajectories for  
 121 up to five years.

122 The UK contact matrix (average daily contacts between an individual in age group  $j$  with individuals in  
 123 age group  $i$ ) comes from a ‘citizen science’ project for the BBC, in which individuals in the UK population  
 124 provided detailed information on their daily contacts in the home, in the workplace, at school and in other  
 125 settings [39, 40]. The contact matrix is altered to account for changes to contact patterns during and after the  
 126 main intervention period [47]. During the lockdown, home; work; school; and other contacts are reduced to 0.8,  
 127 0.3, 0.1 and 0.2 respectively of their baseline values. This reflects the school closures for all children, except  
 128 for those of key workers, and that workers were encouraged to work from home. Reduction in home contacts  
 129 accounts for the absence of visitors to the home during the lockdown. In the post-lockdown phase, home; work;  
 130 school; and other contacts are scaled to 1, 0.8, 0.85 and 0.75, respectively, of their baseline values to reflect  
 131 limited social distancing measures that are likely to be in place until at least the end of 2021.

132 Analysis was performed in R version 3.6.3. We present figures from model output in the text to the nearest  
 133 thousand. Code is available at <https://github.com/tc13/covid-19-immunity>.

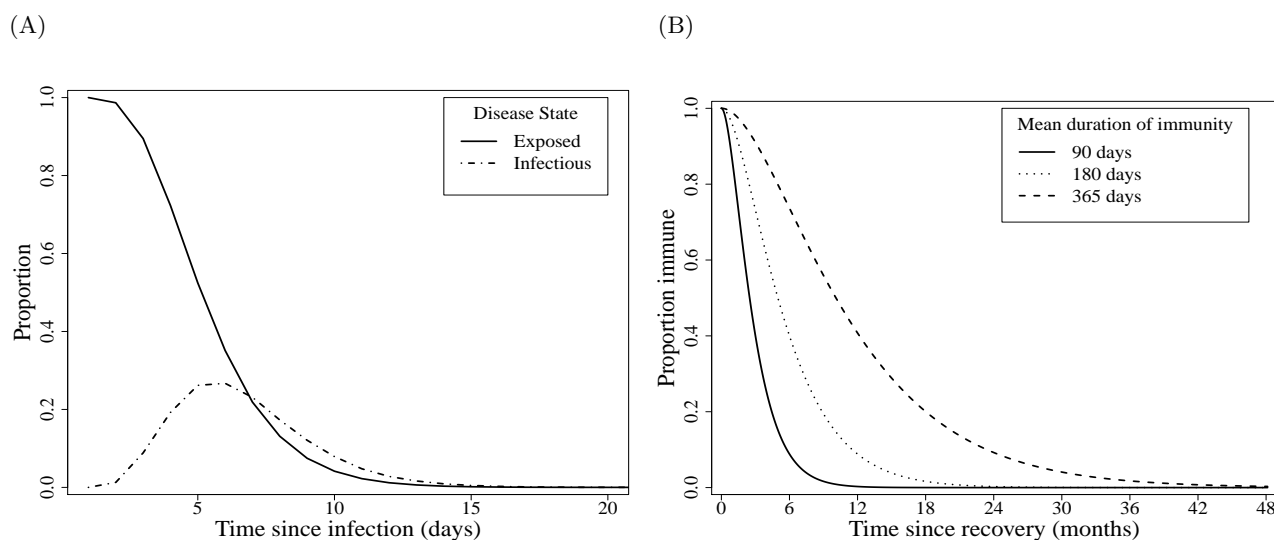


Figure 2: Probabilities for time spent in each state given gamma distributed rates of removal. A. Proportion of individuals in exposed and infectious classes since time from infection. Time exposed and time infectious have mean durations of 3.1 and 4.5 days respectively. B. Proportion of individuals immune since recovery, where time immune has mean durations of 90, 180 or 365 days depending on the scenario.

## 134 Results

### 135 Age structure

136 The epidemic is driven by the rate of infectious contacts between individuals in different age groups. This is  
 137 described by the next generation matrix in which the average number of secondary cases generated by an index  
 138 case in age group  $j$  is the summation of row  $j$  (Equation 8 & Figure 3). At the beginning of the epidemic, when  
 139 SARS-CoV-2 is spreading rapidly, all age groups are involved in transmission; in particular those aged 20–39  
 140 years. An index case in the 20–24 age group, for instance, is expected to generate an average of 3.1 secondary  
 141 cases at baseline. As lockdown measures come into force this dramatically reduces the expected number of  
 142 secondary cases due to fewer contacts and a lower probability of infection given contact. The average number  
 143 of secondary cases from an individual aged 20–24 during lockdown drops to 0.9 and the transmission parameter

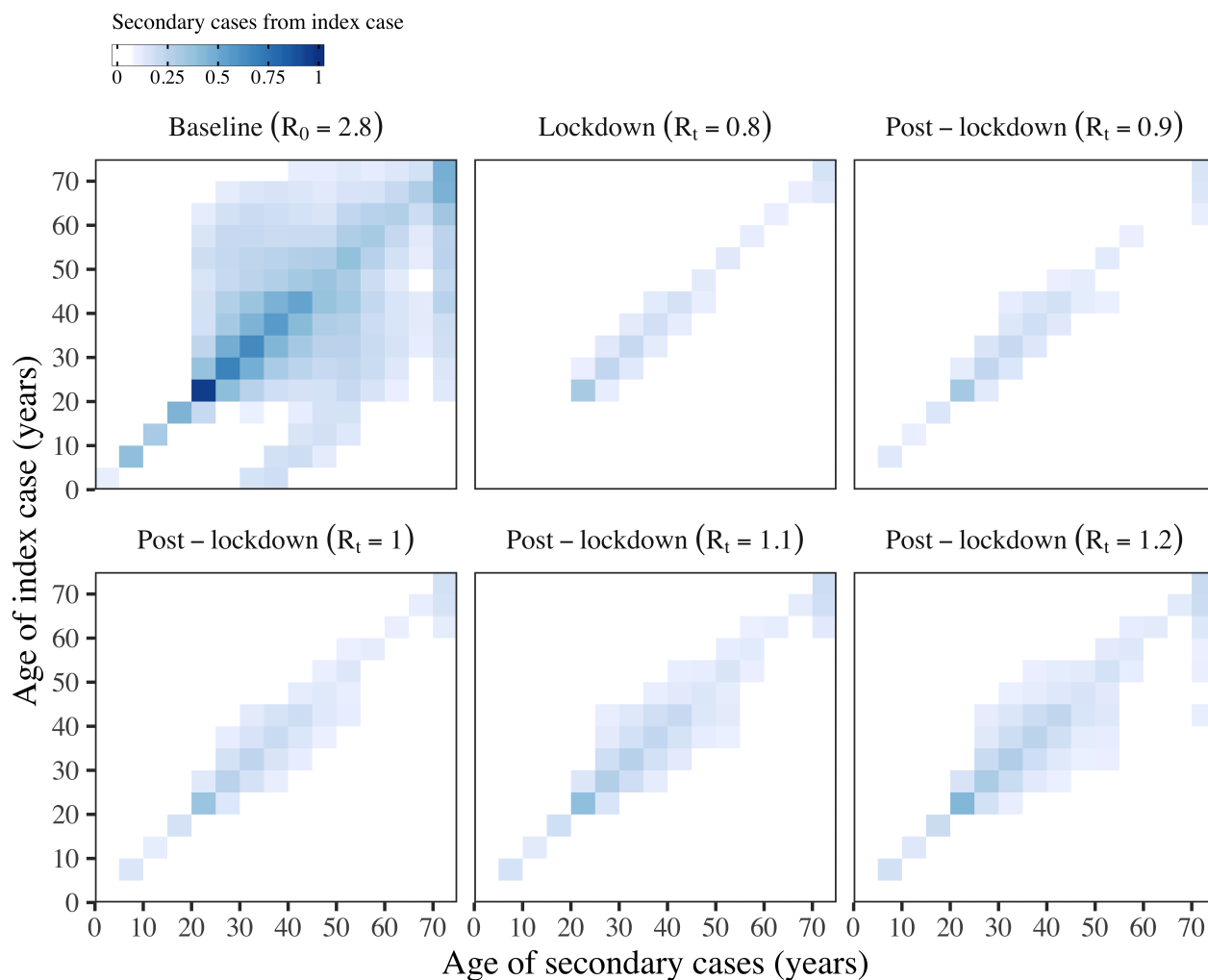


Figure 3: Next generation matrix ( $K = k_{ij}$ ) showing the number of secondary cases generated by an index case from age group  $j$  (rows) in age group  $i$  (columns). The matrices are shown for different time points; at baseline before the implementation of interventions; during the lockdown period; and in the post-lockdown period when the effective reproduction number ( $R_t$ ) rises from 0.9–1.2. The average number of secondary cases generated by an index case from age group  $j$  is the summation of row  $j$ .

144  $\beta$ , which captures the probability of infection given contact, is decreased from 0.13 at baseline to 0.11. In the  
 145 post-lockdown period daily contacts are increased to a higher proportion of their baseline values (see Methods);  
 146 in order to keep the reproduction number equal to the dominant eigenvalue of the next generation matrix,  $\beta$  is  
 147 consequently reduced to 0.05 when  $R_t = 0.9$  and to 0.07 when  $R_t = 1.2$ . This implies that, to maintain  $R_t$  below  
 148 one when more contacts are occurring in the population post-lockdown, the probability that contact results in  
 149 infection will need to be reduced.

## 150 Infection dynamics

151 For the first 130 days until the end of the lockdown, the infection dynamics are equivalent across the four  
 152 immunity scenarios S1–S4 (Figure 4, panels A, C, E & G). After this time the dynamics depend on both the  
 153 rate at which recovered individuals lose immunity and become re-susceptible, and the post-lockdown  $R_t$ .

154 Given our model and parameters, on the first day the intervention is imposed (23<sup>rd</sup> March 2020) there are  
 155 96,000 new SARS-CoV-2 cases, which is within the 95% credible interval (CrI) of new cases estimated for the UK  
 156 on that day (95% CrI 54,000–155,000 [50]), and 124,000 people are infectious (infected compartments  $I^A + I^S$ )  
 157 on this date. From 16<sup>th</sup> February until 23<sup>rd</sup> March there are 717,000 cumulative cases across all age groups and  
 158 680,000 in adults  $\geq 19$  years, which narrowly exceeds the credible interval for an estimate of cumulative cases  
 159 in this period (95% CrI 266,000–628,000 [50]). When most of the lockdown measures were eased in June, 5.5%  
 160 of the total population and 6.8% of adults aged  $\geq 19$  years have immunity to SARS-CoV-2 (in recovered classes  
 161  $R^H$  and  $R^N$ ), which is comparable to estimates of antibody levels in the UK population, estimated as 6.8% of



162 blood donors on 24<sup>th</sup> May 2020 (95% confidence interval 5.2–8.6%; individuals  $\geq 18$  years [25]).

## 163 Secondary peak in infections

164 A secondary peak in infections is expected in spring 2021 where  $R_t = 1.1$  or winter 2020 where  $R_t = 1.2$   
165 (Figure 4, panels E & G). The height of the secondary peak is determined by the rate at which immunity is  
166 lost. In our worst case scenario (S4: short-lived immunity) where immunity lasts an average of three months for  
167 non-hospitalised patients, a year for hospitalised patients and  $R_t$  following lockdown is 1.2, then the secondary  
168 peak will exceed the initial peak with a maximum of 409,000 infectious individuals and 133,000 daily new cases  
169 in December 2020. This is nearly triple the number of new cases compared with scenario S1 where immunity  
170 is permanent; the maximum number of infectious individuals in the secondary peak is 137,000 and there are  
171 45,000 daily new cases (Figure 4G). We note that the timing of the secondary peak in infection curves across  
172 immunological scenarios are closely synchronised and in autumn 2020. This synchrony and timing is also  
173 observed during the epidemic when values of  $R_t$  post-lockdown are greater than 1.2 (explored for values of  $R_t$   
174 from 1.3 to 2.0).

175 When  $R_t$  following lockdown is 1.1, the differences between the scenarios is even more pronounced with a  
176 six-fold difference in the height of the secondary peak of infectious individuals between a scenario of permanent  
177 immunity and one of short-lived immunity. When immunity wanes rapidly, a secondary peak is observed in  
178 April 2021 with a maximum of 161,000 infectious individuals and 52,000 daily new cases. By contrast when  
179 immunity is permanent, the number of new infections slowly decays rather than accelerates, and there are  
180 projected to be only 24,000 infectious individuals and 5,000 daily new cases in April 2021 (Figure 4E).

## 181 Population immunity

182 Dynamics of population immunity (recovered compartments  $R^H + R^N$ ) are similarly shaped by the expected  
183 duration of antibodies against SARS-CoV-2 and the post-lockdown  $R_t$ .

184 Immunity decays from midway through the lockdown period in scenarios S2–S4 of waning (12 or 6 months)  
185 and short-lived immunity and resurges following a secondary wave of infection if  $R_t > 1$  (Figure 4, panels F &  
186 H). After lockdown, a fall in the proportion of the population immune to the virus is observed until autumn 2020  
187 for all values of  $R_t$ , after which point the secondary peak, if  $R_t > 1$ , causes the proportion of the population  
188 immune to rise again. This suggests that longitudinal serological surveys to detect waning immunity would be  
189 most informative when conducted in the period June–September 2020.

## 190 Consequences of age structure

191 The large differences in the heights of the secondary peaks when  $R_t > 1$  between immunological scenarios  
192 (Figure 4, panels A, C, E & G) can be explained by the heterogeneity in transmission (see the next generation  
193 matrix in Figure 3). Infectious and immune cases as a proportion of the total age group are shown in Figure 5  
194 for scenarios S1 & S4 of permanent and short-lived immunity where  $R_t = 1.2$  following lockdown. A higher  
195 proportion of individuals aged between 20–39 are infected early in the epidemic, and this leads to 10.5–12.6%  
196 of individuals in these age groups having antibodies by September 2020 when immunity is life-long (Figure 5B).  
197 When immunity wanes, however, by September 2020 this drops to 5.3–6.6% (Figure 5D), thus increasing the pool  
198 of susceptible individuals to include more of the age groups that drive transmission. This causes the secondary  
199 peak of infectious cases to rise more rapidly and to a greater height when immunity wanes (Figure 5C), compared  
200 with permanent immunity (Figure 5A). Our models suggest that the age distribution of cases in the epidemic  
201 will not change greatly over time; as seen in Figure 5 the ordering of the proportion of each age group infected  
202 remains constant in both scenarios of permanent and short-lived immunity.

## 203 Longer term dynamics: extinction or endemic equilibrium

204 We explored the impact of waning immunity and  $R_t$  on the equilibrium values for the different simulations  
205 over a longer, five year, period until February 2025 (Table 2). If the post-lockdown  $R_t$  is suppressed below  
206 one following lockdown, then the differences in immunity will have less impact on the longer-term infection  
207 dynamics, assuming no imported cases, as transmission of SARS-CoV-2 becomes unsustainable and the virus  
208 reaches extinction between April–November 2021 depending on the immunity scenario. In simulations where  $R_t$   
209 equals one, if immunity is permanent then the epidemic becomes extinct in May 2022. When immunity wanes  
210 there is no secondary peak (Figure 4C), however the infections persist at a low level of endemicity equivalent  
211 to 106, 233 and 1,168 daily cases in immunity scenarios S2–S4, respectively. For larger values of  $R_t$ , and where  
212 immunity wanes, the system oscillates with subsequent peaks of infection over the next five years until a steady  
213 state is reached. We find that, if  $R_t = 1.2$  post-lockdown and immunity is short-lived, there is the potential for  
214 over 76,000 new cases daily; 6,000 hospitalisations; and 1,000 intensive care unit (ICU) admissions (calculated

as 17% of all hospitalised cases [51]) at endemic equilibrium (January 2025), which would be sufficient to overwhelm contact tracing services and ICU capacity [52, 53].

$R_t$ <sup>1</sup>	Immunity scenario <sup>2</sup>	Daily cases <sup>3</sup>	Daily hospitalisations <sup>4</sup>	Daily ICU admissions <sup>5</sup>	Date equilibrium reached <sup>6</sup>
0.9	S1: Permanent	0	0	0	April 2021
	S2: Waning (12 months)	0	0	0	June 2020
	S3: Waning (6 months)	0	0	0	September 2021
	S4: Short-lived	0	0	0	November 2021
1.0	S1: Permanent	0	0	0	May 2022
	S2: Waning (12 months)	106	9	2	After Jan. 2025
	S3: Waning (6 months)	233	20	3	After Jan. 2025
	S4: Short-lived	1,168	100	17	After Jan. 2025
1.1	S1: Permanent	0	0	0	October 2024
	S2: Waning (12 months)	9,354	780	133	After Jan. 2025
	S3: Waning (6 months)	15,268	1,236	210	After Jan. 2025
	S4: Short-lived	41,388	3,489	593	May 2023
1.2	S1: Permanent	0	0	0	October 2022
	S2: Waning (12 months)	23,131	1,906	324	After Jan. 2025
	S3: Waning (6 months)	28,057	2,168	369	After Jan. 2025
	S4: Short-lived	76,307	6,368	1,083	January 2025

Table 2: Values at equilibrium from the modelled scenarios for SARS-CoV-2 in the United Kingdom, explored over a five year horizon (February 2020 to February 2025). <sup>1</sup>Effective reproduction number of SARS-CoV-2 following after lockdown. <sup>2</sup>Assumed duration of immunity for hospitalised and non-hospitalised individuals, see Methods for details of scenarios S1–S4. <sup>3</sup>Number of individuals newly infected with SARS-CoV-2 that enter the exposed  $E$  state. <sup>4</sup>Number of symptomatic individuals with SARS-CoV-2 that enter the recovered hospitalised  $R^H$  state. <sup>5</sup>Number of hospitalised individuals admitted to intensive care units, under the assumption that 17% of hospitalised cases in the UK require care in high dependency units [51]. <sup>6</sup>Either when the number of daily new cases drops below one (extinction), or when the daily new cases are the same integer value over a sustained period (endemic equilibrium). If models take longer than five years to reach a steady state, the values are reported for the last day on 31<sup>st</sup> January 2025.

## Discussion

Despite only 6% of the adult UK population having immunity against SARS-CoV-2 in our simulation at the end of the lockdown, the modelled scenarios suggest that, if this acquired immunity wanes over time, there are substantive differences to the subsequent infection dynamics. Waning immunity impacts on the height of the secondary peak and, in the absence of future interventions, establishes the virus at levels of endemic equilibrium that could overwhelm contact tracing services and ICU capacity [52, 53].

We predict that surveys to detect waning immunity at the population level would be most effective when carried out in the period between the end of lockdown and autumn 2020, as after this point an upsurge in cases is expected that will increase the proportion of the population with antibodies to SARS-CoV-2. In particular, this will allow evaluation of whether specific antibodies generated against the virus are short-lived if reductions in antibody prevalence are observed at the population level.

We find that transmission is driven disproportionately by individuals of working age, and subsequently a higher proportion of individuals aged 20–39 years become infected early in the pandemic and subsequently develop antibodies (Figures 3 & 5). This prediction is borne out by serological data from Switzerland, which showed that individuals aged 20–49 years were significantly more likely to be seropositive in May 2020 compared with younger and older age groups [54]. We postulate that ‘key workers’ in the UK population who have continued to work during the lockdown are more likely to have antibodies against SARS-CoV-2. Higher immunity among individuals of working age has the effect of slowing the subsequent epidemic when immunity is permanent. Conversely, when immunity wanes, previously infected individuals of working age re-join the susceptible pool and so contribute again to transmission; leading to a high growth rate and a larger secondary peak of infected cases. In these circumstances, efforts to suppress transmission will be challenging in the absence of a transmission-blocking vaccine [15]. We note that the model structure developed here is capable of simulating the impact of vaccination with a vaccine that provides temporary transmission-blocking immunity, and could be used to predict the optimal timing for booster shots.



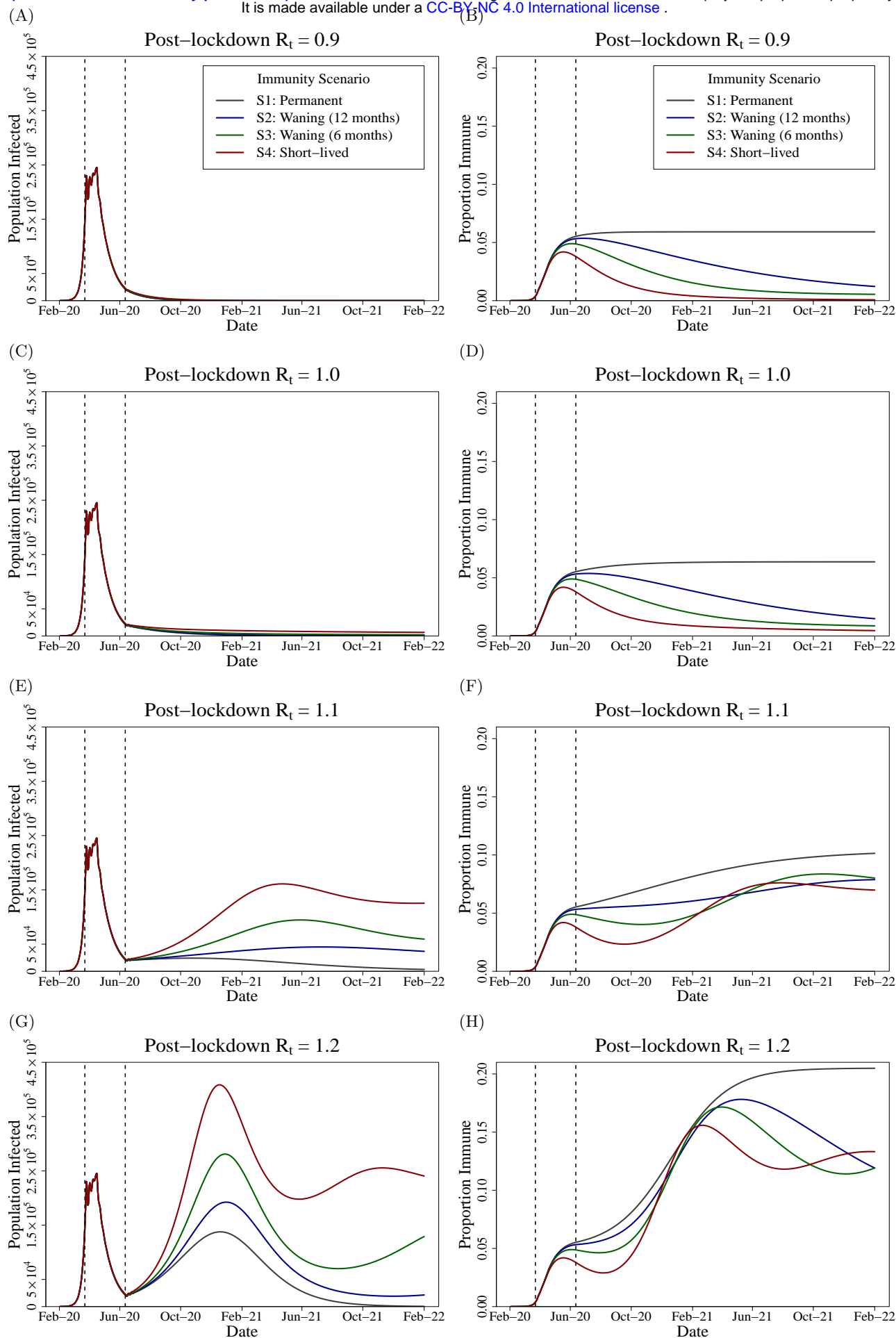


Figure 4: Projections from immunity scenarios S1–4 with post-lockdown  $R_t$  ranging from 0.9–1.2. Left panels show the number of infected, both asymptomatic and symptomatic ( $I^A + I^S$ ), with SARS-CoV-2 in the UK population over time. Right panels show the proportion of the UK population with immunity (compartments  $R^H + R^N$ ). Dashed vertical lines indicate the lockdown period; 23<sup>rd</sup> March–15<sup>th</sup> June 2020.

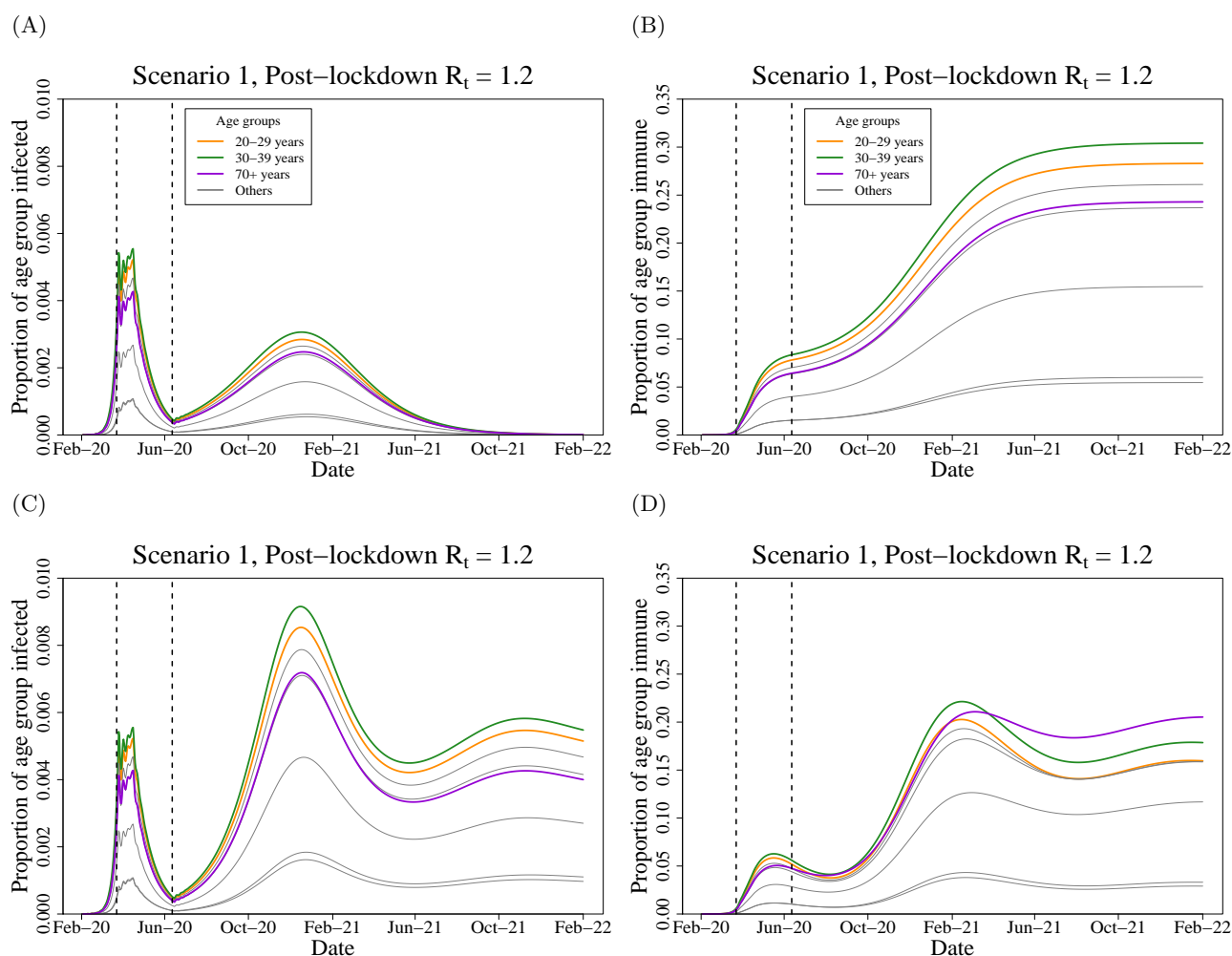


Figure 5: Projections from immunity scenarios S1 & S4 with post-lockdown  $R_t$  of SARS-CoV-2 at 1.2 in the UK population over time. Left panels show the proportion of each age group infected, for both asymptomatic and symptomatic ( $I^A + I^S$ ) individuals. Right panels show the proportion of the each age group with immunity (compartments  $R^H + R^N$ ). Dashed vertical lines indicate the intervention (lockdown) period; 23<sup>rd</sup> March - 15<sup>th</sup> June 2020.

241 The projected trajectory of the epidemic after lockdown is highly sensitive to the effective reproduction  
 242 number, with model behaviour for values of  $R_t$  slightly above or below one displaying qualitatively different  
 243 dynamics (Figure 4). This shows the importance of timely and accurate estimates of  $R_t$  to inform control  
 244 strategies, and ensuring widespread community testing and contact tracing is in place. Our calculations show  
 245 that to suppress  $R_t$  below one when contact rates rise to a higher fraction of baseline (pre-lockdown) values,  
 246 the probability of infection given contact (represented here by the  $\beta$  parameter), must drop by around half.  
 247 Interventions that have the potential to reduce the probability of infection include social distancing; regular  
 248 hand washing; and the wearing of face masks outside the home [55].

249 Our study reinforces the importance of better understanding SARS-CoV-2 immunity among recovered in-  
 250 dividuals of different ages and disease severity. In scenarios where immunity wanes and  $R_t$  following lockdown  
 251 is greater than one, the SARS-CoV-2 epidemic never reaches extinction due to herd immunity, but rather the  
 252 number of infected cases oscillates with subsequent waves of infection before reaching endemic equilibrium (Ta-  
 253 ble 2). Even in simulations where the reproduction number only narrowly exceeds one, if immunity wanes over  
 254 an average of one year for severe cases and three months for non-severe cases, this is projected to lead to an  
 255 equilibrium state of over 40,000 daily new cases and 200 daily admissions to intensive care. Policy strategies  
 256 aiming to achieve herd immunity are therefore risky [5], as if SARS-CoV-2 antibodies do wane over time, then  
 257 a herd immunity threshold can never be reached in the absence of a vaccine that provides permanent immunity  
 258 [21]. The establishment of an endemic equilibrium state is dependent on no future interventions or changes to  
 259  $R_t$ , which we consider unlikely as policy makers and public health agencies are likely to react to future outbreaks  
 260 with localised control measures.

261 One of the strengths of our study is that the model is calibrated to key features of the UK epidemic. While  
 262 we did not explicitly fit to data, new cases at the start of the lockdown; cumulative cases between February

263 and March; and the proportion of the adult population with antibodies to SARS-CoV-2 are highly comparable  
264 between our output and current estimates [25, 50]. We used contact matrices from a comprehensive study  
265 of contact patterns in the UK population [39] in addition to demographic data from the Office for National  
266 Statistics, to give our simulations the best chance of capturing realistic age-specific transmission patterns in the  
267 UK population.

268 Plausible estimates on which to base expectations for the duration of immunity are sparse in the current  
269 literature. Rosado *et al.* estimated that antibodies could wane in 50% of recovered individuals after one year  
270 [48], which is similar to the estimated duration of immunity against seasonal circulating coronaviruses [13]. Even  
271 with this consideration, there are many probability distributions that can be used to capture a median duration  
272 of immunity, and our selection of an Erlang distribution with a shape parameter of two is somewhat arbitrary.  
273 Our assumptions on the duration of the latent and infectious periods are more closely informed by estimates from  
274 data [29, 46, 47]. We made the decision to capture the expected duration of these states as Erlang distributions  
275 rather than the, more conventional, exponential distribution. This has the benefit of closely replicating fitted  
276 gamma or log-normal distributions within a compartmental model [30], and has important implications for the  
277 dynamics of the epidemic [56, 57]. We make a number of assumptions regarding the natural history of the  
278 virus, such as the relative susceptibility of children compared with adults and the relative infectiousness of  
279 symptomatic versus asymptomatic cases based on the current literature [44, 41]. Future empirical studies are  
280 likely to add to and further refine these epidemiological parameters. After we completed the analysis, a study of  
281 37 asymptomatic individuals in China were found to have a longer period of viral shedding when compared with  
282 symptomatic individuals [10]. While viral shedding is not necessarily indicative of transmission potential [7], if  
283 these findings are replicated in larger studies this may suggest a need to use different durations of infectiousness  
284 for asymptomatic and symptomatic infections in subsequent models.

285 We have aimed to capture future infection dynamics at a national level in the UK under a range of scenarios.  
286 Our analysis is limited by not considering regional differences in transmission rates, for instance through a patch  
287 (metapopulation) model [40], or a stochastic approach that allows for local extinction events [21]. There are  
288 no deaths in our model, either from demography or infection. Accounting for mortality would mainly affect  
289 dynamics in the oldest age group (over 70 years) [16, 51], as the higher probability of disease-induced mortality  
290 would prevent a substantial build up of immunity (Figure 5D). We also do not explicitly consider transmission  
291 in settings such as hospitals or care homes, although such dynamics may be captured indirectly through the  
292 contact matrix. Given the simplicity of the model structure, we advise against treating the output as an exact  
293 prediction of the future. In addition to the limitations listed above, the epidemic trajectory will be substantially  
294 altered by any future interventions such as a return to full lockdown conditions, or intensive contact tracing  
295 and isolation [13, 58].

## 296 Acknowledgements

297 This work was undertaken as a contribution to the Rapid Assistance in Modelling the Pandemic (RAMP)  
298 initiative, coordinated by the Royal Society. The authors thank Prof. Julia Gog and Dr. Rosalind Eggo for  
299 their helpful comments and input.

## 300 Disclosure statement

301 The authors declare no conflicts of interest. No other authors have been paid to write this article.

## 302 Open access

303 Anyone can share and adapt this article provided they give credit and link to this article's DOI and CC BY 4.0  
304 licence ([creativecommons.org/licenses/by/4.0](https://creativecommons.org/licenses/by/4.0/)).

## 305 Funding

306 TC is funded by a Sir Henry Wellcome Postdoctoral Fellowship from the Wellcome Trust (reference 215919/Z/19/Z).  
307 ELD, TCDL, DA, AB, TMP and TDH gratefully acknowledge funding of the NTD Modelling Consortium by  
308 the Bill & Melinda Gates Foundation (BMGF) (grant number OPP1184344). Views, opinions, assumptions or  
309 any other information set out in this article should not be attributed to BMGF or any person connected with  
310 them. TMP's PhD was supported by the Engineering & Physical Sciences Research Council, Medical Research  
311 Council and University of Warwick (grant number EP/L015374/1). All funders had no role in the study de-  
312 sign, collection, analysis, interpretation of data, writing of the report, or decision to submit the manuscript for  
313 publication.

## References

- 314
- 315 [1] Worldometer. Covid-19 data. <https://www.worldometers.info/coronavirus/>, June 2020.
- 316 [2] Esteban Ortiz-Ospina Max Roser, Hannah Ritchie and Joe Hasell. Our World in Data. Coronavirus  
317 (COVID-19) cases. <https://ourworldindata.org/covid-cases>, June 2020.
- 318 [3] Kristian G. Andersen, Andrew Rambaut, W. Ian Lipkin, Edward C. Holmes, and Robert F. Garry. The  
319 proximal origin of SARS-CoV-2. *Nature Medicine*, 26(4):450–452, 2020.
- 320 [4] UK Government. Coronavirus (COVID-19) in the uk. <https://coronavirus.data.gov.uk/>, June 2020.
- 321 [5] Heba Habib. Has Sweden’s controversial covid-19 strategy been successful? *BMJ*, 369, 2020.
- 322 [6] Quan-Xin Long, Bai-Zhong Liu, Hai-Jun Deng, Gui-Cheng Wu, Kun Deng, Yao-Kai Chen, Pu Liao, Jing-  
323 Fu Qiu, Yong Lin, Xue-Fei Cai, et al. Antibody responses to SARS-CoV-2 in patients with COVID-19.  
324 *Nature Medicine*, pages 1–4, 2020.
- 325 [7] Roman Wölfel, Victor M. Corman, Wolfgang Guggemos, Michael Seilmaier, Sabine Zange, Marcel A.  
326 Müller, Daniela Niemeyer, Terry C. Jones, Patrick Vollmar, Camilla Rothe, et al. Virological assessment  
327 of hospitalized patients with COVID-2019. *Nature*, pages 1–5, 2020.
- 328 [8] Linlin Bao, Wei Deng, Hong Gao, Chong Xiao, Jiayi Liu, Jing Xue, Qi Lv, Jiangning Liu, Pin Yu, Yanfeng  
329 Xu, et al. Lack of reinfection in rhesus macaques infected with SARS-CoV-2. *bioRxiv*, 2020.
- 330 [9] Juanjuan Zhao, Quan Yuan, Haiyan Wang, Wei Liu, Xuejiao Liao, Yingying Su, Xin Wang, Jing Yuan,  
331 Tingdong Li, Jinxiu Li, et al. Antibody responses to SARS-CoV-2 in patients of novel coronavirus disease  
332 2019. *Clinical Infectious Diseases*, 2020.
- 333 [10] Quan-Xin Long, Xiao-Jun Tang, Qiu-Lin Shi, Qin Li, Hai-Jun Deng, Jun Yuan, Jie-Li Hu, Wei Xu, Yong  
334 Zhang, Fa-Jin Lv, et al. Clinical and immunological assessment of asymptomatic SARS-CoV-2 infections.  
335 *Nature Medicine*, pages 1–5, 2020.
- 336 [11] Wu-Chun Cao, Wei Liu, Pan-He Zhang, Fang Zhang, and Jan H. Richardus. Disappearance of antibodies  
337 to sars-associated coronavirus after recovery. *New England Journal of Medicine*, 357(11):1162–1163, 2007.
- 338 [12] Pyoeng Gyun Choe, R. A. P. M. Perera, Wan Beom Park, Kyoung-Ho Song, Ji Hwan Bang, Eu Suk Kim,  
339 Hong Bin Kim, Long Wei Ronald Ko, Sang Won Park, Nam-Joong Kim, et al. MERS-CoV antibody  
340 responses 1 year after symptom onset, South Korea, 2015. *Emerging Infectious Diseases*, 23(7):1079, 2017.
- 341 [13] Stephen M. Kissler, Christine Tedijanto, Edward Goldstein, Yonatan H. Grad, and Marc Lipsitch. Pro-  
342 jecting the transmission dynamics of SARS-CoV-2 through the postpandemic period. *Science*, 2020.
- 343 [14] Patience K. Kiyuka, Charles N. Agoti, Patrick K. Munywoki, Regina Njeru, Anne Bett, James R. Otieno,  
344 Grieven P. Otieno, Everlyn Kamau, Taane G. Clark, Lia van der Hoek, et al. Human coronavirus n163  
345 molecular epidemiology and evolutionary patterns in rural coastal Kenya. *The Journal of Infectious Dis-  
346 eases*, 217(11):1728–1739, 2018.
- 347 [15] Paul Kellam and Wendy Barclay. The dynamics of humoral immune responses following SARS-CoV-2  
348 infection and the potential for reinfection. *Journal of General Virology*, page jgv001439, 2020.
- 349 [16] Neil Ferguson, Daniel Laydon, Gemma Nedjati Gilani, Natsuko Imai, Kylie Ainslie, Marc Baguelin,  
350 Sangeeta Bhatia, Adhiratha Boonyasiri, Zulma Cucunuba Perez, Gina Cuomo-Dannenburg, et al. Re-  
351 port 9: Impact of non-pharmaceutical interventions (NPIs) to reduce COVID19 mortality and healthcare  
352 demand. 2020.
- 353 [17] Adam J. Kucharski, Timothy W. Russell, Charlie Diamond, Yang Liu, John Edmunds, Sebastian Funk,  
354 Rosalind M. Eggo, Fiona Sun, Mark Jit, James D. Munday, et al. Early dynamics of transmission and  
355 control of COVID-19: a mathematical modelling study. *The Lancet Infectious Diseases*, 2020.
- 356 [18] Kiesha Prem, Yang Liu, Timothy W. Russell, Adam J. Kucharski, Rosalind M. Eggo, Nicholas Davies,  
357 Stefan Flasche, Samuel Clifford, Carl A. B. Pearson, James D. Munday, et al. The effect of control  
358 strategies to reduce social mixing on outcomes of the COVID-19 epidemic in Wuhan, China: a modelling  
359 study. *The Lancet Public Health*, 2020.
- 360 [19] T Déirdre Hollingsworth, Don Klinkenberg, Hans Heesterbeek, and Roy M Anderson. Mitigation strategies  
361 for pandemic influenza a: balancing conflicting policy objectives. *PLoS Comput Biol*, 7(2):e1001076, 2011.

- 362 [20] M. Gabriela M. Gomes, Lisa J. White, and Graham F. Medley. Infection, reinfection, and vaccination under  
363 suboptimal immune protection: epidemiological perspectives. *Journal of Theoretical Biology*, 228(4):539–  
364 549, 2004.
- 365 [21] Matt J Keeling and Pejman Rohani. *Modeling infectious diseases in humans and animals*. Princeton  
366 University Press, 2011.
- 367 [22] Henrik Salje, Cécile Tran Kiem, Noémie Lefrancq, Noémie Courtejoie, Paolo Bosetti, Juliette Paireau,  
368 Alessio Andronico, Nathanaël Hozé, Jehanne Richet, Claire-Lise Dubost, et al. Estimating the burden of  
369 SARS-CoV-2 in France. *Science*, 2020.
- 370 [23] Seth Flaxman, Swapnil Mishra, Axel Gandy, H Juliette T Unwin, Thomas A Mellan, Helen Coupland,  
371 Charles Whittaker, Harrison Zhu, Tresnia Berah, Jeffrey W Eaton, et al. Estimating the effects of non-  
372 pharmaceutical interventions on COVID-19 in Europe. *Nature*, pages 1–8, 2020.
- 373 [24] Alessia Lai, Annalisa Bergna, Carla Acciarri, Massimo Galli, and Gianguglielmo Zehender. Early phy-  
374 logenetic estimate of the effective reproduction number of SARS-CoV-2. *Journal of Medical Virology*,  
375 92(6):675–679, 2020.
- 376 [25] Office for National Statistics. Coronavirus (COVID-19) Infection Survey pilot: 28 May 2020. Technical  
377 report, 2020.
- 378 [26] Roy M. Anderson and Robert M. May. *Infectious Diseases of Humans: Dynamics and Control*. Oxford  
379 University Press, 1992.
- 380 [27] M. Gabriela M. Gomes, Ricardo Aguas, Rodrigo M. Corder, Jessica G. King, Kate E. Langwig, Caetano  
381 Souto-Maior, Jorge Carneiro, Marcelo U. Ferreira, and Carlos Penha-Goncalves. Individual variation in  
382 susceptibility or exposure to SARS-CoV-2 lowers the herd immunity threshold. *medRxiv*, 2020.
- 383 [28] Tom Britton, Frank Ball, and Pieter Trapman. The disease-induced herd immunity level for Covid-19 is  
384 substantially lower than the classical herd immunity level. *arXiv preprint arXiv:2005.03085*, 2020.
- 385 [29] Xi He, Eric H. Y. Lau, Peng Wu, Xilong Deng, Jian Wang, Xinxin Hao, Yiu Chung Lau, Jessica Y. Wong,  
386 Yujuan Guan, Xinghua Tan, et al. Temporal dynamics in viral shedding and transmissibility of COVID-19.  
387 *Nature Medicine*, pages 1–4, 2020.
- 388 [30] Helen J. Wearing, Pejman Rohani, and Matt J. Keeling. Appropriate models for the management of  
389 infectious diseases. *PLoS Medicine*, 2(7), 2005.
- 390 [31] James O. Lloyd-Smith, Alison P. Galvani, and Wayne M. Getz. Curtailing transmission of severe acute  
391 respiratory syndrome within a community and its hospital. *Proceedings of the Royal Society of London.*  
392 *Series B: Biological Sciences*, 270(1528):1979–1989, 2003.
- 393 [32] Steven Riley, Christophe Fraser, Christl A Donnelly, Azra C Ghani, Laith J Abu-Raddad, Anthony J  
394 Hedley, Gabriel M Leung, Lai-Ming Ho, Tai-Hing Lam, Thuan Q Thach, et al. Transmission dynamics of  
395 the etiological agent of SARS in Hong Kong: impact of public health interventions. *Science*, 300(5627):1961–  
396 1966, 2003.
- 397 [33] Christopher I Jarvis, Kevin Van Zandvoort, Amy Gimma, Kiesha Prem, Petra Klepac, G James Rubin, and  
398 W John Edmunds. Quantifying the impact of physical distance measures on the transmission of COVID-19  
399 in the UK. *BMC Medicine*, 18:1–10, 2020.
- 400 [34] J Kucharski Adam, Klepac Petra, JK Andrew, M Kissler Stephen, L Tang Maria, Fry Hannah, R Julia,  
401 CMMID COVID-19 working group, et al. Effectiveness of isolation, testing, contact tracing, and physical  
402 distancing on reducing transmission of SARS-CoV-2 in different settings: A mathematical modelling study.  
403 *The Lancet Infectious Diseases*, pages S1473–3099, 2020.
- 404 [35] Enrico Lavezzo, Elisa Franchin, Constanze Ciavarella, Gina Cuomo-Dannenburg, Luisa Barzon, Claudia  
405 Del Vecchio, Lucia Rossi, Riccardo Manganelli, Arianna Loregian, Nicolò Navarin, et al. Suppression of  
406 COVID-19 outbreak in the municipality of Vo, Italy. *medRxiv*, 2020.
- 407 [36] Robert Verity, Lucy C Okell, Ilaria Dorigatti, Peter Winskill, Charles Whittaker, Natsuko Imai, Gina  
408 Cuomo-Dannenburg, Hayley Thompson, Patrick GT Walker, Han Fu, et al. Estimates of the severity of  
409 coronavirus disease 2019: a model-based analysis. *The Lancet Infectious Diseases*, 2020.
- 410 [37] Kenji Mizumoto, Katsushi Kagaya, Alexander Zarebski, and Gerardo Chowell. Estimating the asymp-  
411 tomatic proportion of coronavirus disease 2019 (COVID-19) cases on board the Diamond Princess cruise  
412 ship, Yokohama, Japan, 2020. *Eurosurveillance*, 25(10):2000180, 2020.



- 413 [38] C. Li, F. Ji, L. Wang, J. Hao, M. Dai, Y. Liu, X. Pan, J. Fu, L. Li, G. Yang, et al. Asymptomatic and  
414 human-to-human transmission of SARS-CoV-2 in a 2-family cluster, Xuzhou, China. *Emerging Infectious*  
415 *Diseases*, 26(7), 2020.
- 416 [39] Petra Klepac, Stephen Kissler, and Julia Gog. Contagion! The BBC Four Pandemic—the model behind  
417 the documentary. *Epidemics*, 24:49–59, 2018.
- 418 [40] Petra Klepac, Adam J. Kucharski, Andrew J. K. Conlan, Stephen Kissler, Maria Tang, Hannah Fry,  
419 and Julia R. Gog. Contacts in context: large-scale setting-specific social mixing matrices from the BBC  
420 Pandemic project. *medRxiv*, 2020.
- 421 [41] Nicholas G. Davies, Petra Klepac, Yang Liu, Kiesha Prem, Mark Jit, CMMID COVID-19 working group  
422 Eggo, Rosalind M., et al. Age-dependent effects in the transmission and control of COVID-19 epidemics.  
423 *Nature Medicine*, 2020.
- 424 [42] Juanjuan Zhang, Maria Litvinova, Yuxia Liang, Yan Wang, Wei Wang, Shanlu Zhao, Qianhui Wu, Stefano  
425 Merler, Cecile Viboud, Alessandro Vespignani, et al. Age profile of susceptibility, mixing, and social  
426 distancing shape the dynamics of the novel coronavirus disease 2019 outbreak in China. *medRxiv*, 2020.
- 427 [43] Daniel F. Gudbjartsson, Agnar Helgason, Hakon Jonsson, Olafur T. Magnusson, Pall Melsted, Gud-  
428 mundur L. Norddahl, Jona Saemundsdottir, Asgeir Sigurdsson, Patrick Sulem, Arna B. Agustsdottir, et al.  
429 Spread of SARS-CoV-2 in the Icelandic population. *New England Journal of Medicine*, 2020.
- 430 [44] Qin-Long Jing, Ming-Jin Liu, Zhou-Bin Zhang, Li-Qun Fang, Jun Yuan, An-Ran Zhang, Natalie E Dean,  
431 Lei Luo, Meng-Meng Ma, Ira Longini, et al. Household secondary attack rate of COVID-19 and associated  
432 determinants in Guangzhou, China: a retrospective cohort study. *The Lancet Infectious Diseases*, 2020.
- 433 [45] Jiuxin Qu, Chi Wu, Xiaoyong Li, Guobin Zhang, Zhaofang Jiang, Xiaohe Li, Lei Liu, et al. Profile of  
434 IgG and IgM antibodies against severe acute respiratory syndrome coronavirus 2 (SARS-CoV-2). *Clinical*  
435 *Infectious Diseases*, 2020.
- 436 [46] Qun Li, Xuhua Guan, Peng Wu, Xiaoye Wang, Lei Zhou, Yeqing Tong, Ruiqi Ren, Kathy SM Leung,  
437 Eric HY Lau, Jessica Y Wong, et al. Early transmission dynamics in wuhan, china, of novel coronavirus-  
438 infected pneumonia. *New England Journal of Medicine*, 2020.
- 439 [47] Nicholas G Davies, Adam J Kucharski, Rosalind M Eggo, Amy Gimma, W John Edmunds, Thibaut  
440 Jombart, Kathleen O'Reilly, Akira Endo, Joel Hellewell, Emily S Nightingale, et al. Effects of non-  
441 pharmaceutical interventions on COVID-19 cases, deaths, and demand for hospital services in the UK:  
442 a modelling study. *The Lancet Public Health*, 2020.
- 443 [48] Jason Rosado, Charlotte Cockram, Sarah Helene Merklung, Caroline Demeret, Annalisa Meola, Solen  
444 Kerneis, Benjamin Terrier, Samira Fafi-Kremer, Jerome de Seze, Marija Backovic, et al. Serological signa-  
445 tures of SARS-CoV-2 infection: Implications for antibody-based diagnostics. *medRxiv*, 2020.
- 446 [49] Centre for the Mathematical Modelling of Infectious Disases, London School of Hygiene  
447 and Tropical Medicine. Temporal variation in transmission during the COVID-19 outbreak.  
448 <https://epiforecasts.io/covid/>, June 2020.
- 449 [50] Mark Jit, Thibaut Jombart, Emily S. Nightingale, Akira Endo, Sam Abbott, L.S.H.T.M. Centre for Math-  
450 ematical Modelling of Infectious Diseases COVID-19 Working Group, and W. John Edmunds. Estimating  
451 number of cases and spread of coronavirus disease (COVID-19) using critical care admissions, United  
452 Kingdom, February to March 2020. *Eurosurveillance*, 25(18), 2020.
- 453 [51] Annemarie B. Docherty, Ewen M. Harrison, Christopher A. Green, Hayley E. Hardwick, Riinu Pius, Lisa  
454 Norman, Karl A. Holden, Jonathan M. Read, Frank Dondelinger, Gail Carson, et al. Features of 20 133 UK  
455 patients in hospital with covid-19 using the ISARIC WHO Clinical Characterisation Protocol: prospective  
456 observational cohort study. *BMJ*, 369, 2020.
- 457 [52] NHS England. Monthly critical care beds and cancelled urgent operations (MSITREP) data,  
458 England. [https://www.england.nhs.uk/statistics/wp-content/uploads/sites/2/2020/04/MSitRep-SPN-](https://www.england.nhs.uk/statistics/wp-content/uploads/sites/2/2020/04/MSitRep-SPN-FEBRUARY-2020-auY71.pdf)  
459 [FEBRUARY-2020-auY71.pdf](https://www.england.nhs.uk/statistics/wp-content/uploads/sites/2/2020/04/MSitRep-SPN-FEBRUARY-2020-auY71.pdf), April 2020.
- 460 [53] Emma L Davis, Tim CD Lucas, Anna Borlase, Timothy M Pollington, Sam Abbott, Diepreye Ayabina,  
461 Thomas Crellen, Joel Hellewell, Li Pi, Graham F Medley, et al. An imperfect tool: COVID-19 'test &  
462 trace' success relies on minimising the impact of false negatives and continuation of physical distancing.  
463 *medRxiv*, 2020.

- 464 [54] Silvia Stringhini, Ania Wisniak, Giovanni Piumatti, Andrew S Azman, Stephen A Lauer, H el ene Baysson,  
465 David De Ridder, Dusan Petrovic, Stephanie Schrepft, Kailing Marcus, et al. Seroprevalence of anti-  
466 SARS-CoV-2 IgG antibodies in Geneva, Switzerland (SEROCoV-POP): a population-based study. *The*  
467 *Lancet*, 2020.
- 468 [55] Benjamin J Cowling and Allison E Aiello. Public health measures to slow community spread of coronavirus  
469 disease 2019. *The Journal of Infectious Diseases*, 221(11):1749–1751, 2020.
- 470 [56] Alun L Lloyd. Realistic distributions of infectious periods in epidemic models: changing patterns of  
471 persistence and dynamics. *Theoretical population biology*, 60(1):59–71, 2001.
- 472 [57] AC Fowler and T D eirdre Hollingsworth. Simple approximations for epidemics with exponential and fixed  
473 infectious periods. *Bulletin of mathematical biology*, 77(8):1539–1555, 2015.
- 474 [58] Joel Hellewell, Sam Abbott, Amy Gimma, Nikos I Bosse, Christopher I Jarvis, Timothy W Russell, James D  
475 Munday, Adam J Kucharski, W John Edmunds, Fiona Sun, et al. Feasibility of controlling COVID-19  
476 outbreaks by isolation of cases and contacts. *The Lancet Global Health*, 2020.